

Published in final edited form as:

Hepatology. 2013 January ; 57(1): 385–398. doi:10.1002/hep.26016.

Monocyte Subsets in Human Liver Disease Show Distinct Phenotypic and Functional Characteristics

Evaggelia Liaskou¹, Henning W. Zimmermann^{1,2}, Ka-Kit Li¹, Ye H. Oo¹, Shankar Suresh¹, Zania Stamataki¹, Omar Qureshi³, Patricia F. Lalor¹, Jean Shaw¹, Wing-kin Syn^{1,4,5}, Stuart M. Curbishley¹, and David H. Adams¹

¹Centre for Liver Research and NIHR Biomedical Research Unit in Liver Disease, Institute of Biomedical Research, University of Birmingham, Birmingham, United Kingdom

²Medical Department III, University Hospital of Aachen, Germany

³Medical Research Council Centre for Immune Regulation, School of Immunity and Infection, Institute of Biomedical Research, University of Birmingham Medical School, Birmingham, United Kingdom

⁴The Institute of Hepatology, Regeneration and Repair Group, London, United Kingdom

⁵Department of Physiology, University of the Basque Country, Bilbao, Spain

Abstract

Liver fibrosis is a wound healing response to chronic liver injury and inflammation in which macrophages and infiltrating monocytes participate in both the development and resolution phase. In humans, three monocyte subsets have been identified: the classical CD14⁺⁺CD16⁻, intermediate CD14⁺⁺CD16⁺, and nonclassical CD14⁺CD16⁺⁺ monocytes. We studied the phenotype and function of these monocyte subsets in peripheral blood and liver tissue from patients with chronic inflammatory and fibrotic liver diseases. The frequency of intrahepatic monocytes increased in disease compared with control liver tissue, and in both nondiseased and diseased livers there was a higher frequency of CD14⁺⁺CD16⁺ cells with blood. Our data suggest two nonexclusive mechanisms of CD14⁺⁺CD16⁺ accumulation in the inflamed liver: (1) recruitment from blood, because more than twice as many CD14⁺⁺CD16⁺ monocytes underwent transendothelial migration through hepatic endothelial cells compared with CD14⁺⁺CD16⁻ cells; and (2) local differentiation from CD14⁺⁺CD16⁻ classical monocytes in response to transforming growth factor β and interleukin (IL)-10. Intrahepatic CD14⁺⁺CD16⁺ cells expressed both macrophage and dendritic cell markers but showed high levels of phagocytic activity, antigen presentation, and T cell proliferation and secreted proinflammatory (tumor necrosis factor α , IL-6, IL-8, IL-1 β) and profibrogenic cytokines (IL-13), chemokines (CCL1, CCL2, CCL3, CCL5), and growth factors (granulocyte colony-stimulating factor and granulocyte-macrophage colony-stimulating factor), consistent with a role in the wound healing response.

Copyright © 2012 by the American Association for the Study of Liver Diseases.

Address reprint requests to: David H. Adams, Professor of Hepatology, Centre for Liver Research, 5th Floor 1BR, University of Birmingham, Edgbaston, Birmingham B152TT, United Kingdom. d.h.adams@bham.ac.uk; fax: (44)-121-415-8701.

Potential conflict of interest: Nothing to report.

Conclusion—Intermediate CD14⁺⁺CD16⁺ monocytes preferentially accumulate in chronically inflamed human liver as a consequence of enhanced recruitment from blood and local differentiation from classical CD14⁺⁺CD16[–] monocytes. Their phagocytic potential and ability to secrete inflammatory and profibrogenic cytokines suggests they play an important role in hepatic fibrogenesis.

Chronic, progressive liver disease is characterized by fibrogenesis, cirrhosis, and hepatocellular carcinoma.¹ These characteristics are driven by persistent inflammation arising from liver cell injury and a dysregulated tissue repair response. Current medical therapies are limited, and liver transplantation is the only curative treatment for individuals with end-stage liver disease. Hence, better understanding of the inflammatory mechanisms that modulate fibrogenesis will be important for the development of future therapies aimed at inhibiting or reversing liver disease progression.

Liver fibrosis shares many features with wound healing responses. Although activated hepatic stellate cells (HSCs) are responsible for the majority of the extracellular matrix deposition,² immune cells including CD8 T lymphocytes,³ natural killer (NK) T cells,⁴ and NK cells^{5,6} all shape the local microenvironment during fibrogenesis. Recent studies suggest an important role for monocytes and their tissue progeny macrophages in fibrogenesis. Duffield et al.⁷ implicated liver macrophages in fibrosis progression and resolution, suggesting that functionally distinct subpopulations participate in the different phases of fibrogenesis. These findings were further corroborated by subsequent studies emphasizing the phase-dependent consequences of monocyte-derived macrophages.⁸ In line with this study, reducing liver-infiltrating macrophages was found to attenuate fibrosis in some models,⁹ and it has been suggested that recruited monocytes are the major mediators of liver fibrogenesis, with liver resident Kupffer cells playing only a minor role.¹⁰ The apparent functional differences between infiltrating monocytes and resident macrophages remain poorly understood but could be explained by the hypothesis that monocytes recruited from the blood in response to inflammation differentiate into functionally distinct monocyte and macrophage subsets within the liver. Depending on their state of differentiation and local signals, monocytes and macrophages are capable of secreting a variety of proinflammatory, profibrotic, and anti-inflammatory cytokines and growth factors.¹¹ The function of monocytes in the liver may be the consequence of different processes: (1) hepatic monocytes and macrophages are shaped by microenvironmental signals to differentiate into cells that either promote fibrosis progression or enhance fibrosis resolution, and (2) circulating monocytes preprogrammed with defined pro- or antifibrotic properties are recruited to the liver at different time points and act locally according to their inherent program.

In humans, the major population of monocytes (~90%) expresses high levels of CD14 but no CD16 (CD14⁺⁺CD16[–]) and are now termed classical monocytes.¹² The minor population (~10%) of human monocytes is further subdivided into the intermediate subset, with high CD14 and low CD16 (CD14⁺⁺CD16⁺), and the nonclassical subset with low CD14 and high CD16 (CD14⁺CD16⁺⁺).¹² *In vitro* and *in vivo* studies suggest that these subsets differ in cytokine secretion and adhesion molecule and chemokine receptor expression^{13,14}; however, their differential role in chronic liver disease remains largely unknown.

In order to understand the role of infiltrating monocytes in liver inflammation, we studied the phenotype and function of the three monocyte subsets in peripheral blood and liver tissue of patients with different chronic inflammatory/fibrotic liver diseases. We present evidence that implicates the intermediate monocyte subset in the pathogenesis of liver fibrosis. We propose that the accumulation of these cells in the liver is a consequence of local transdifferentiation from classical CD14⁺⁺CD16⁻ monocytes and preferential recruitment from the circulation via inflamed sinusoidal endothelium.

Patients and Methods

Human Tissue and Blood

Human liver tissue was obtained through the Liver Unit at the Queen Elizabeth Hospital (Birmingham, UK). Diseased liver came from a variety of patients with end-stage liver disease; nondiseased liver came from either donor tissue surplus to transplantation requirements or from uninvolved liver tissue removed from surgical resections of liver tissue containing metastatic tumors. Whole blood was obtained from healthy volunteers and from patients with liver diseases. Whole blood was also obtained from patients undergoing liver transplantation just prior to transplantation for autologous T cell proliferation experiments. All human tissue and blood samples were collected with local research ethics committee approval and patient consent.

Isolation of Liver-Infiltrating Mononuclear Cells

Liver-infiltrating mononuclear cells were isolated from fresh human liver tissue according to a methodology established by our group¹⁵ and as described in the Supporting Information.

Bead-Sorted and Fluorescence-Activated Cell-Sorted Monocyte Subsets and Hepatic Dendritic Cells

Monocyte subsets from peripheral blood and liver were isolated using the CD16⁺ Monocyte isolation kit and CD14 Microbeads (Miltenyi Biotec) according to the manufacturer's instructions (Supporting Information). Using this technique, we could isolate the classical monocytes to >95% purity; however, due to difficulties in obtaining the intermediate and nonclassical subsets separately (Supporting Fig. 1), for the functional experiments throughout this study, two groups were studied: the CD14⁺⁺CD16⁻ and the CD14⁺CD16⁺ (or CD16).

Cell sorting was also used to acquire hepatic dendritic cells (DCs) and monocyte subsets from both peripheral blood and liver. Monocytes were defined by the expression of CD14 and CD16 markers and exclusion of CD3⁺ lymphocytes, CD19⁺ B cells, CD66b⁺ granulocytes, and CD56⁺ NK cells. Liver DCs were defined as CD14⁻CD16⁻CD3⁻CD56⁻CD66b⁻CD19⁻HLA-DR^{hi} cells.

Isolation of Peripheral Blood Mononuclear Cells and CD4⁺ T cells

Peripheral blood mononuclear cells were isolated from human peripheral blood, following established methodology¹³ described in the Supporting Information. CD4 T cells were

isolated from peripheral blood mononuclear cells using magnetic CD4 beads (Miltenyi Biotec) according to the manufacturer's instructions, labeled with 2 μ M carboxyfluorescein succinimidyl ester (CFSE; Invitrogen) and incubated overnight at 37°C prior to coculturing with liver-infiltrating monocytes and DCs.

Antigen Presentation and Autologous T Cell Proliferation

Liver-infiltrating monocyte subsets and DCs were isolated from explanted liver (primary biliary cirrhosis [PBC] and alcoholic liver disease [ALD]) using a fluorescence-activated cell sorting (FACS) technique and were incubated with *tuberculosis* protein (2,000 U per 10⁶ cells) for 24 hours prior to coculturing with CFSE-labeled autologous CD4⁺ T cells for 4 days at 1:1, 1:2, 1:5, 1:10, and 1:50 ratios (monocyte/DC:CD4) in Roswell Park Memorial Institute 1640 medium (RPMI-1640)/10% fetal bovine serum. T cell proliferation was studied via flow cytometry.

Isolation and Culture of Human Hepatic Sinusoidal Endothelial Cells

Hepatic sinusoidal endothelial cells were isolated from approximately 150 g of liver tissue as described.¹⁶ The isolation procedure is described in the Supporting Information.

Flow Cytometry

Flow cytometric analysis was performed on blood and liver-derived mononuclear cells using a CyAn flow cytometer (Beckman Coulter, Bucks, UK). The procedure and antibodies used are described in the Supporting Information and Supporting Table 1. FlowJo version 7 software was employed for data analysis. The induction of CD16 expression on CD14⁺CD16⁻ subset after *in vitro* cytokine stimulation was also verified using flow cytometry. Peripheral blood CD14⁺⁺CD16⁻ monocytes were stimulated with tumor necrosis factor α (TNF α) (Peprotech; 10 ng/mL), interferon- γ (IFN γ ; Peprotech; 10 ng/mL), interleukin (IL)-4 and IL-13 (Miltenyi Biotec; 10ng/ml), IL-10 (Miltenyi Biotec; 50 ng/mL), transforming growth factor β (TGF β) (Peprotech; 5 ng/mL) and combinations of cytokines for 1, 3, and 5 days prior to analysis of CD16 expression. IL-10 and TGF β were tested at different concentrations (5-50 ng/mL) with no difference in their ability to induce CD16 expression.

Flow-Based Adhesion Assays

The ability of monocyte subsets to migrate across hepatic sinusoidal endothelial cells (HSECs) was studied using flow-based adhesion assays.¹⁷ In brief, monolayers of HSECs were cultured until confluency in Ibidi microslides (5 μ -Slide VI^{0.4}; Thistle Scientific) and stimulated for 24 hours with TNF α and IFN γ (both at 10 ng/mL; Peprotech) prior to perfusion of peripheral blood monocyte subsets at a wall shear stress of 0.05 Pa mimicking intrasinusoidal flow conditions. Adherent cells were visualized using phase contrast microscopy (\times 10 objective) and classified as rolling, static, or migrated. Total adhesion and transmigration were calculated as cells per mm² normalized to a million monocytes perfused.

Immunohistochemical Analysis

Multicolor-fluorescence confocal microscopy was used to localize the expression of monocyte subsets in human liver tissue. Protocol and antibodies used are described in the Supporting Information and Supporting Table 2.

Monocyte-Conditioned Media

Liver-infiltrating monocyte subsets (CD14⁺⁺CD16⁻ and CD14⁺CD16⁺) were isolated as described above and were cultured in RPMI-1640/10% fetal bovine serum for 48 hours at 37°C. The cell suspension was collected, centrifuged and the cell-free conditioned media was collected and stored in smaller aliquots at -80°C for further cytokine secretion analysis.

Cytokine Secretion Assays

The secretion of a variety of cytokines from liver-derived monocyte subsets (CD14⁺CD16⁻ and CD14⁺CD16⁺) was tested using cytokine array panel A kit (Invitrogen) according to the manufacturer's instructions.

Phagocytosis Assays

Liver-infiltrating and peripheral blood monocyte subsets (CD14⁺⁺CD16⁻ and CD14⁺CD16⁺) were tested for their ability to phagocytose unopsonized Zymosan A BioParticles (Molecular Probes, Invitrogen). The assay is based on the fluorescence of fluorescein-labeled bioparticles, which is quenched in an acidic environment. The amount of phagocytosis thus was determined by examining the quenched zymosan inside monocytes using real-time confocal imaging (Zeiss LSM 780 Zen).

Statistical Analyses

Data were analyzed using a Student *t* test when comparing numerical variables between two groups and one-way analysis of variance followed by Bonferroni's post-test for comparisons between more than two groups. Statistical analyses were performed using GraphPad Prism software. *P* < 0.05 was considered statistically significant.

Results

Increased Numbers of Monocytes Are Detected in Diseased Human Livers

We first analyzed total monocyte frequencies in nondiseased human liver obtained from organ donors or uninvolved tissue removed at hepatic resection and compared these results with diseased livers [ALD, nonalcoholic steatohepatitis (NASH), PBC and primary sclerosing cholangitis (PSC)] removed at transplantation. Monocytes were defined by their size and granularity in forward and side scatter plots and by the expression of CD14 and CD16 after exclusion of CD56⁺CD16⁺ NK cells and CD66b⁺CD16⁺ granulocytes (Fig. 1A, 1). As expected diseased livers contained more leukocytes than nondiseased liver and flow cytometric analysis revealed that a greater proportion of the liver-infiltrating leukocytes were monocytes in diseased livers (11.57% ± 0.94 SEM; n = 34) compared with nondiseased livers (8.67% ± 0.88 SEM; n = 17) (*P* = 0.02) (Fig. 1A,2). When we analyzed specific etiologies, we observed a two-fold increase in the proportion of monocytes in

alcoholic and nonalcoholic liver diseases (ALD/NASH livers [14.46% \pm 1.16 SEM; n = 20]) compared with nondiseased livers (8.67% \pm 0.88 SEM; n = 17) ($P = 0.0002$) (Fig. 1A,3). In contrast, monocyte frequencies in cholestatic liver diseases were not different from nondiseased livers (PBC/PSC livers; 7.44 \pm 0.71 SEM; n = 14) (Fig. 1A,3).

CD16+ Monocytes Preferentially Accumulate in Diseased Human Liver

Next, we compared monocyte subset (classical, intermediate, and nonclassical) (Fig. 1B) frequencies in the peripheral blood and livers of normal controls and patients with liver disease. The CD14⁺⁺CD16⁻ classical subset constituted approximately 80% of peripheral blood mononuclear cells (MNCs) in both healthy controls and in patients with liver disease, but only 50% of MNCs in nondiseased and diseased livers. There was a statistically significant difference between nondiseased liver and normal peripheral blood ($P = 0.005$) and between diseased liver and diseased peripheral blood from patients with chronic liver disease ($P < 0.0001$) (Fig. 1C, left panel).

A significant reduction of CD14⁺⁺CD16⁻ frequencies was observed in all diseases (ALD/NASH and cholestatic liver diseases [PBC/PSC]) (Fig. 1C, right panel). In contrast, the intermediate CD14⁺⁺CD16⁺ subset comprised 9% and 14% of MNCs in normal and diseased peripheral blood, respectively, but was significantly higher (27%) in both nondiseased ($P = 0.0023$) and diseased livers ($P = 0.0007$) (Fig. 1D, left panel). Increased frequencies of the CD14⁺⁺CD16⁺ subset were seen in livers from all etiologies (ALD/NASH and cholestatic liver diseases [PBC/PSC]) (Fig. 1D, right panel) compared with their levels in the peripheral blood of patients with the same disease. There were comparable numbers of nonclassical CD14⁺CD16⁺⁺ cells in healthy blood and liver (11% and 16%, respectively) but higher frequencies in diseased liver compared with blood from patients with the same liver disease (17% diseased liver versus 8% diseased peripheral blood; $P = 0.011$) (Fig. 1E, left panel). Highest frequencies of nonclassical monocytes were detected in liver tissue from patients with cholestatic liver diseases compared to the blood of patients with the same disease ($P = 0.007$) (Fig. 1E, right panel). Finally, we studied the differences between nondiseased donor and resection livers regarding the percentage of monocytes in the total liver-infiltrating MNC population and the percentage of three monocyte subsets (Fig. 1F). We observed a significantly higher ($P = 0.03$) frequency of intermediate monocytes in organ donors compared with resections.

CD16+ Monocytes Show Increased Transendothelial Migration Across Human Hepatic Sinusoidal Endothelial Cells Under Flow Compared With Classical Monocytes In Vitro

Cell cycle studies confirmed that all monocytes in blood and liver were in G zero phase, in a quiescent state where they are not dividing and thus not proliferating (data not shown), suggesting that local proliferation cannot explain the higher frequencies of the CD16⁺ subset in the inflamed liver. To determine whether accumulation in diseased livers was the consequence of an enhanced ability to enter the liver from blood via hepatic endothelium, we studied monocyte transendothelial migration across inflamed hepatic sinusoidal endothelium *in vitro*. Both CD14⁺⁺CD16⁻ and CD14⁺CD16⁺ monocytes bound to untreated HSECs under flow, and the numbers increased 4.37-fold ($P = 0.02$) and 7.49-fold ($P = 0.02$), respectively, when TNF α /IFN γ cytokine-activated HSECs were used (Fig. 2A).

Despite binding, very few of the CD14⁺⁺CD16⁻ and CD14⁺CD16⁺ monocyte subsets underwent transendothelial migration on unstimulated HSECs (Fig. 2B). However, when cytokine-treated endothelial cells were used, a significant proportion of the adherent CD14⁺CD16⁻ and CD14⁺CD16⁺ monocytes underwent transmigration (a 25.8- and 59.8-fold increase in transmigration, respectively) ($P = 0.02$) (Fig. 2B). Twice as many CD14⁺CD16⁺ monocytes underwent transmigration when compared with CD14⁺⁺CD16⁻ monocytes ($P = 0.023$) (Fig. 2C,D). When FACS monocyte subsets were used comparable results were obtained, with intermediate and nonclassical monocytes showing more adhesion and transmigration on hepatic endothelial cells compared with classical monocytes (Fig. 2E). Thus, our data suggest that an enhanced ability to transmigrate across hepatic endothelium from blood into liver tissue accounts in part for the increased proportion of CD16⁺ (CD14⁺CD16⁺ and CD14⁺CD16⁺⁺) monocytes in diseased liver.

CD14⁺⁺CD16⁺ Intermediate Subset Can Be Derived from CD14⁺⁺CD16⁻ Classical Subset

Another explanation for the enrichment of the CD14⁺⁺CD16⁺ subset in the liver is that CD14⁺⁺ monocytes acquire CD16 in response to differentiation signals present in the inflamed liver (i.e., CD14⁺⁺CD16⁺ monocytes are an intermediate subset between classical and nonclassical monocytes).^{18,19} In support of this, we were able to induce the surface expression of CD16 on classical CD14⁺⁺CD16⁻ monocytes simply by culturing them on plastic *in vitro*. The levels of CD16 were further modulated *in vitro* by culturing cells in the presence of T helper (Th) 1 (TNF α and/or IFN γ), Th2 (IL-4 and/or IL-13), or anti-inflammatory (TGF β or IL-10) cytokines for 1, 3, and 5 days (Fig. 3A-D). The Th1 cytokine TNF α reduced CD16 expression, whereas TGF β and IL-10 both enhanced CD16 acquisition. TGF β induced a 2.3-fold increase in the expression of CD16 after 3 and 5 days, IL-10 a 3.3-, 3.1-, and 2.5-fold increase after 1, 3, and 5 days, respectively, compared with the levels of CD16 expression acquired on CD14⁺⁺CD16⁻ monocytes without stimulation (control) (Fig. 3D). IFN γ had no effect, whereas TNF α and IL-4 resulted in repression of spontaneous CD16 up-regulation by 2.4- to 3.6-fold after 1, 3, and 5 days, respectively, for TNF α and 1.5- to 2.7-fold for IL-4. IL-13 had very modest effects, and the combination of IL-4 with IL-13 and of IL-4, IL-10, and IL-13 had no additive effect (Fig. 3D). These data suggest that classical CD14⁺⁺CD16⁻ monocytes can undergo intrahepatic differentiation to express CD16 in response to IL-10 and TGF β in the injured liver microenvironment.

Liver-Infiltrating CD14⁺⁺CD16⁺ Monocytes Exhibit both Macrophage and DC Phenotypes

Having shown that CD14⁺⁺CD16⁺ intermediate monocytes accumulate in the diseased liver, we investigated their phenotype and functional characteristics. Monocytes circulate in blood for several days before migrating into tissues, where they differentiate into tissue macrophages or DCs.²⁰ Liver intermediate CD14⁺⁺CD16⁺ monocytes freshly isolated from both nondiseased and diseased livers and analyzed via flow cytometry exhibited both macrophage characteristics (high levels of CD163, a surface marker predominantly found on alternatively activated M2 macrophages) and DC phenotypic characteristics (high levels of HLA-DR, CD80, CD86, and CD83). All these receptors were expressed at much higher levels on intermediate monocytes compared with classical and nonclassical monocytes (Fig. 4A,B). Flow cytometry histograms revealed the presence of two distinct populations with

lower and higher expression of the DC markers, suggesting the presence of monocytes that may already be committed to macrophage or DC differentiation (Fig. 4A).

To analyze these cells *in situ*, we performed confocal microscopy and three-color immunofluorescent staining of liver tissue for CD14, CD16, and CD68 and confirmed coexpression of CD14, CD16, and CD68 on a population of large cells with the morphology of macrophages that were present throughout the liver sinusoids (Fig. 5A,D). CD14+CD68– and CD16+CD68– cells (Fig. 5B,C) as well as CD14+CD68+ and CD16+CD68+ (Fig. 5A,D; white arrows) were also detected, confirming that distinct monocyte-derived and sessile macrophage populations coexist in the liver.

To define the function of the different monocyte subsets, we tested the ability of both peripheral blood and liver-infiltrating cells to phagocytose zymosan bioparticles. Both CD14++CD16– and CD14+ CD16+ subsets from either peripheral blood or liver were able to phagocytose. However, only 20% of CD14++CD16– and CD14+CD16+ subsets isolated from nondiseased liver were able to phagocytose when compared with the higher proportion (33%) of both subsets in normal peripheral blood (Fig. 6A). In diseased livers, an even lower proportion of CD14+CD16+ monocytes (16%) were phagocytic compared with 30% of CD14++CD16– monocytes from the same diseased livers (Fig. 6A). Although a lower proportion of liver-derived monocytes showed phagocytic activity, both CD14++CD16– and CD14+CD16+ monocytes from nondiseased and diseased livers had higher phagocytic capacity than peripheral blood monocytes when normalized to the number of engulfed particles (Fig. 6B-D). Liver-derived CD14+CD16+ monocytes phagocytosed significantly more zymosan particles than CD14++CD16– from the same liver (Fig. 6B). These data demonstrate the plasticity of CD14+CD16+ monocytes that either become DCs or macrophages in the liver.

Liver-Infiltrating Intermediate and Nonclassical Monocytes Are Antigen-Presenting Cells

To investigate whether liver-infiltrating monocytes are antigen presenting cells, we studied their ability to present *tuberculosis* antigenic peptides to autologous CD4+ T cells. Liver-infiltrating intermediate and nonclassical monocytes (total CD16+) were more efficient at antigen presentation and inducing T cell proliferation compared with classical CD14+CD16– monocytes (Fig. 7A,B). Levels of proliferation with CD16+ monocytes were comparable to those seen with liver-derived DCs. Only a proportion of CD4+ T cells proliferated, consistent with reactivation of memory T cells (Fig. 7B). Our data show that liver-infiltrating CD16+ monocytes display plasticity being able to differentiate into either phagocytic macrophages or antigen-presenting cells capable of activating T cells.

Liver-Infiltrating CD16+ Monocytes Demonstrate

Increased Cytokine Secretion. When cultured *in vitro* for 48 hours without exogenous cytokines or growth factors monocytes from diseased liver tissue secreted higher levels of many cytokines when compared with monocytes from normal blood (data not shown) or nondiseased livers (Fig. 8). Liver-infiltrating CD14+ CD16+ monocytes secreted higher levels of chemokines (CCL1, CCL2, CCL3, CCL5, growth-regulated oncogene α /CXCL1, and CXCL8/IL-8), cytokines (IL-1 α , IL-1 β , IL-6, IL-13, IL-16, TNF α and macrophage

migration inhibitory factor), growth factors (granulocyte colony-stimulating factor and granulocyte-macrophage colony-stimulating factor) and the complement component C5a compared with CD14⁺⁺CD16⁻ monocytes (Fig. 8A-C). Thus, in an inflamed microenvironment, CD16⁺ monocytes are highly activated and secrete higher levels of cytokines and chemokines.

Discussion

Although macrophages have been associated with both the induction and resolution of fibrosis,⁷ it is not known whether distinct macrophage subpopulations are responsible for these divergent processes. Peripheral blood monocytes constantly enter the liver to replenish hepatic macrophages, and the numbers of infiltrating monocytes increase during liver inflammation and modulate fibrogenesis.⁹⁻¹¹ We now show that the CD14⁺⁺CD16⁺ intermediate subset of human monocytes preferentially accumulates in the diseased liver as a consequence of enhanced recruitment from blood and local differentiation from CD14⁺CD16⁻ classical monocytes. Furthermore, intrahepatic CD14⁺⁺CD16⁺ monocytes display plasticity and include cells with macrophage and DC like features. They are able to act as phagocytes and antigen-presenting cells and secrete cytokines and chemokines that will modulate fibrogenesis.¹⁴

Our data suggest that the accumulation of CD14⁺⁺CD16⁺ intermediate monocytes in human liver is the consequence of increased transmigration from blood across hepatic endothelium and local differentiation from classical CD14⁺⁺CD16⁻ monocytes in the presence of TGF β and IL-10. A significantly larger proportion of the CD16⁺ subset adhered to hepatic sinusoidal endothelium under physiological conditions of flow, and of those adherent cells, a significantly higher proportion underwent transendothelial migration across cytokine-activated hepatic endothelium in flow-based adhesion assays. Thus, recruitment will favor the CD16⁺ subset, and over time this will result in enhanced accumulation of these cells within the inflamed liver.

In addition to recruitment, it is also likely that some CD16⁺ cells within the liver are derived from the CD14⁺⁺ classical subset in response to local signals that drive differentiation to the intermediate and nonclassical subset. This is consistent with our confocal analysis of inflamed human liver tissue, which revealed the presence within the livers of CD14⁺CD16⁺, CD14⁺CD16⁻, and CD16⁺CD14⁻ monocytes. We found that IL-10 and TGF β —both of which are present at high local levels in the chronically inflamed liver as a result of secretion by Kupffer cells, macrophages, and infiltrating lymphocytes—promote the expression of CD16 on CD14⁺⁺CD16⁻ monocytes during culture *in vitro*. These data favor a model in which at least some of the CD16⁺ cells are derived from CD14⁺⁺ classical monocytes, suggesting that local differentiation also contributes.^{21,22} Whether CD16⁺ cells that are recruited from blood and those that differentiate within the inflamed environment differ functionally is not known.

We found that liver-infiltrating intermediate monocytes express the scavenger receptor CD163, one of the most reliable markers of M2 macrophages.²³ Many of the intrahepatic CD163⁺CD14⁺⁺CD16⁺ cells also expressed CD68, a marker of tissue resident

macrophages, and macrophage differentiation was confirmed by their ability to phagocytose zymosan particles. M2 macrophages are implicated in inflammation resolution, tissue repair, and fibrogenesis,²⁴ suggesting that the CD14⁺⁺CD16⁺ cells we detected in the liver include a profibrogenic macrophage subset. However, a proportion of liver-infiltrating intermediate monocytes expressed cell surface receptors more consistent with a DC phenotype and were able to present antigen efficiently to autologous CD4⁺ T cells, further confirming their plasticity. These data are consistent with recent findings demonstrating monocyte plasticity²⁵ and suggest that their ultimate differentiation and function will be closely related to the inflammatory microenvironment within the liver.

We suggest that intrahepatic CD14⁺CD16⁺ monocytes are major modulators of fibrogenesis. They secreted cytokines and chemokines that are implicated in fibrogenesis, including TNF α , IL-6, CXCL8/IL-8, CXCL1, CCL2, CCL3, CCL5, and IL-13. CCL2 is a profibrogenic chemokine that is highly up-regulated in injured liver, where it plays a role in the recruitment of monocytes/macrophages that are associated with HSC activation and liver fibrosis.^{7,26} *In vivo* studies have shown that inactivation of CCL2 reduces CCl₄-induced liver injury and fibrosis⁹ and that deficiency of the CCL2 receptor CCR2 also attenuates liver inflammation and fibrosis.^{8,27} CCL3 and CCL5 are increased during fibrogenesis, and inactivation of their receptors CCR1 and CCR5 results in reduced hepatic fibrosis in animal models.²⁸ CXCR1 and CXCR2 are expressed on both resting and activated HSCs and contribute to the establishment of a profibrogenic microenvironment in chronic liver disease.²⁹ Apart from direct interaction with HSCs, CCL2, CCL5, CXCL1, and CXCL8 also augment the recruitment of inflammatory cells and promote a profibrotic microenvironment within the inflamed liver. TNF α is an important activator of HSCs,³⁰ and treatment with Infliximab, an anti-TNF α agent, attenuates fibrosis in response to CCl₄-induced liver injury in rats.³¹ IL-6 promotes fibroblast proliferation, collagen production, and tissue inhibitor of metalloproteinase-1 synthesis,³² and numerous studies in animal models demonstrate the importance of IL-13 in fibrogenesis.^{33,34}

It is known that infiltrating monocytes and resident macrophages play a critical role in the resolution of inflammation and subsequent tissue repair by clearing necrotic/apoptotic cells and promoting angiogenesis and the recruitment of regulatory cells that secrete anti-inflammatory cytokines and growth factors such as IL-10 and TGF β .²² These cascades result in matrix remodeling and repair of tissues. Our data showing that in the presence of the immunosuppressive cytokines IL-10 and TGF β , classical monocytes differentiate into cells with both macrophage and DC-like characteristics, is consistent with this model and represents one in which their dysregulation leads to uncontrolled inflammation and scar formation characteristics of chronic inflammation.

In conclusion, we have identified features that distinguish monocyte subsets from the inflamed liver and suggest that the intermediate subset can modulate liver fibrogenesis and is thus a potential therapeutic target in chronic inflammatory liver disease.

Supplementary Material

Refer to Web version on PubMed Central for supplementary material.

Acknowledgments

We are grateful to the sponsors of this work, Wellcome Trust, the NIHR Liver BRU, EASL, BRET, CORE and Royal Society Dorothy Hodgkin. We would also like to thank Dr Nicholas Davies for his technical advice on cell cycle assays and Mrs Bridget Gunson for her advice on statistical analyses.

This work was supported by grants from the Wellcome Trust, The Medical Research Council and the National Institute for Health Research (NIHR) Birmingham Liver Biomedical Research Unit based at University Hospital Birmingham NHS Foundation Trust and the University of Birmingham. The views expressed are those of the author(s) and not necessarily those of the NHS, the NIHR or the Department of Health. HWZ was supported by the 'Rotationsprogramm' of the Medical Faculty of the University of Aachen.

Abbreviations

ALD	alcoholic liver disease
CFSE	carboxyfluorescein succinimidyl ester
DC	dendritic cell
FACS	fluorescence-activated cell sorting
HSC	hepatic stellate cell
HSEC	hepatic sinusoidal endothelial cell
IFNγ	interferon- γ
IL	interleukin
MNC	mononuclear cell
NASH	nonalcoholic steatohepatitis
NK	natural killer
PBC	primary biliary cirrhosis
PSC	primary sclerosing cholangitis
RPMI-1640	Roswell Park Memorial Institute 1640 medium
TGFβ	transforming growth factor β
Th	T helper
TNFα	tumor necrosis factor α

References

1. Fleming KM, Aithal GP, Solaymani-Dodaran M, Card TR, West J. Incidence and prevalence of cirrhosis in the United Kingdom, 1992-2001: a general population-based study. *J Hepatol.* 2008; 49:732-738. [PubMed: 18667256]
2. Moreira RK. Hepatic stellate cells and liver fibrosis. *Arch Pathol Lab Med.* 2007; 131:1728-1734. [PubMed: 17979495]
3. Safadi R, Ohta M, Alvarez CE, Fiel MI, Bansal M, Mehal WZ, et al. Immune stimulation of hepatic fibrogenesis by CD8 cells and attenuation by transgenic interleukin-10 from hepatocytes. *Gastroenterology.* 2004; 127:870-882. [PubMed: 15362042]
4. Park O, Jeong WI, Wang L, Wang H, Lian ZX, Gershwin ME, et al. Diverse roles of invariant natural killer T cells in liver injury and fibrosis induced by carbon tetrachloride. *Hepatology.* 2009; 49:1683-1694. [PubMed: 19205035]

5. Radaeva S, Sun R, Jaruga B, Nguyen VT, Tian Z, Gao B. Natural killer cells ameliorate liver fibrosis by killing activated stellate cells in NKG2D-dependent and tumor necrosis factor-related apoptosis-inducing ligand-dependent manners. *Gastroenterology*. 2006; 130:435–452. [PubMed: 16472598]
6. Melhem A, Muhanna N, Bishara A, Alvarez CE, Ilan Y, Bishara T, et al. Anti-fibrotic activity of NK cells in experimental liver injury through killing of activated HSC. *J Hepatol*. 2006; 45:60–71. [PubMed: 16515819]
7. Duffield JS, Forbes SJ, Constandinou CM, Clay S, Partolina M, Vuthoori S, et al. Selective depletion of macrophages reveals distinct, opposing roles during liver injury and repair. *J Clin Invest*. 2005; 115:56–65. [PubMed: 15630444]
8. Mitchell C, Couton D, Couty JP, Anson M, Crain AM, Bizet V, et al. Dual role of CCR2 in the constitution and the resolution of liver fibrosis in mice. *Am J Pathol*. 2009; 174:1766–1775. [PubMed: 19359521]
9. Imamura M, Ogawa T, Sasaguri Y, Chayama K, Ueno H. Suppression of macrophage infiltration inhibits activation of hepatic stellate cells and liver fibrogenesis in rats. *Gastroenterology*. 2005; 128:138–146. [PubMed: 15633130]
10. Karlmark KR, Weiskirchen R, Zimmermann HW, Gassler N, Ginhoux F, Weber C, et al. Hepatic recruitment of the inflammatory Gr1+ monocyte subset upon liver injury promotes hepatic fibrosis. *Hepatology*. 2009; 50:261–274. [PubMed: 19554540]
11. Bataller R, Brenner DA. Liver fibrosis. *J Clin Invest*. 2005; 115:209–218. [PubMed: 15690074]
12. Ziegler-Heitbrock L, Ancuta P, Crowe S, Dalod M, Grau V, Hart DN, et al. Nomenclature of monocytes and dendritic cells in blood. *Blood*. 2010; 116:e74–80. [PubMed: 20628149]
13. Aspinall AI, Curbishley SM, Lalor PF, Weston CJ, Blahova M, Liaskou E, et al. CX(3)CR1 and vascular adhesion protein-1-dependent recruitment of CD16(+) monocytes across human liver sinusoidal endothelium. *Hepatology*. 2010; 51:2030–2039. [PubMed: 20512991]
14. Zimmermann HW, Seidler S, Nattermann J, Gassler N, Hellerbrand C, Zerneck A, et al. Functional contribution of elevated circulating and hepatic non-classical CD14CD16 monocytes to inflammation and human liver fibrosis. *PLoS One*. 2010; 5:e11049. [PubMed: 20548789]
15. Eksteen B, Miles A, Curbishley SM, Tselepis C, Grant AJ, Walker LS, et al. Epithelial inflammation is associated with CCL28 production and the recruitment of regulatory T cells expressing CCR10. *J Immunol*. 2006; 177:593–603. [PubMed: 16785557]
16. Liaskou E, Karikoski M, Reynolds GM, Lalor PF, Weston CJ, Pullen N, et al. Regulation of mucosal addressin cell adhesion molecule 1 expression in human and mice by vascular adhesion protein 1 amine oxidase activity. *Hepatology*. 2011; 53:661–672. [PubMed: 21225644]
17. Lalor PF, Sun PJ, Weston CJ, Martin-Santos A, Wakelam MJ, Adams DH. Activation of vascular adhesion protein-1 on liver endothelium results in an NF-kappaB-dependent increase in lymphocyte adhesion. *Hepatology*. 2007; 45:465–474. [PubMed: 17256751]
18. Wong HL, Welch GR, Brandes ME, Wahl SM. IL-4 antagonizes induction of Fc gamma RIII (CD16) expression by transforming growth factor-beta on human monocytes. *J Immunol*. 1991; 147:1843–1848. [PubMed: 1653804]
19. Kruger M, Coorevits L, De Wit TP, Casteels-Van Daele M, Van De Winkel JG, Ceuppens JL. Granulocyte-macrophage colony-stimulating factor antagonizes the transforming growth factor-beta-induced expression of Fc gamma RIII (CD16) on human monocytes. *Immunology*. 1996; 87:162–167. [PubMed: 8666430]
20. Tacke F, Randolph GJ. Migratory fate and differentiation of blood monocyte subsets. *Immunobiology*. 2006; 211:609–618. [PubMed: 16920499]
21. Knolle P, Schlaak J, Uhrig A, Kempf P, Meyer zum Buschenfelde KH, Gerken G. Human Kupffer cells secrete IL-10 in response to lipopolysaccharide (LPS) challenge. *J Hepatol*. 1995; 22:226–229. [PubMed: 7790711]
22. Heymann F, Trautwein C, Tacke F. Monocytes and macrophages as cellular targets in liver fibrosis. *Inflamm Allergy Drug Targets*. 2009; 8:307–318. [PubMed: 19534673]
23. Kawamura K, Komohara Y, Takaishi K, Katabuchi H, Takeya M. Detection of M2 macrophages and colony-stimulating factor 1 expression in serous and mucinous ovarian epithelial tumors. *Pathol Int*. 2009; 59:300–305. [PubMed: 19432671]

24. Wynn TA, Barron L. Macrophages: master regulators of inflammation and fibrosis. *Semin Liver Dis.* 2010; 30:245–257. [PubMed: 20665377]
25. Rivollier A, He J, Kole A, Valatas V, Kelsall BL. Inflammation switches the differentiation program of Ly6Chi monocytes from antiinflammatory macrophages to inflammatory dendritic cells in the colon. *J Exp Med.* 2012; 209:139–155. [PubMed: 22231304]
26. Marra F, DeFranco R, Grappone C, Milani S, Pastacaldi S, Pinzani M, et al. Increased expression of monocyte chemotactic protein-1 during active hepatic fibrogenesis: correlation with monocyte infiltration. *Am J Pathol.* 1998; 152:423–430. [PubMed: 9466568]
27. Seki E, de Minicis S, Inokuchi S, Taura K, Miyai K, van Rooijen N, et al. CCR2 promotes hepatic fibrosis in mice. *Hepatology.* 2009; 50:185–197. [PubMed: 19441102]
28. Seki E, De Minicis S, Gwak GY, Kluwe J, Inokuchi S, Bursill CA, et al. CCR1 and CCR5 promote hepatic fibrosis in mice. *J Clin Invest.* 2009; 119:1858–1870. [PubMed: 19603542]
29. Zimmermann HW, Seidler S, Gassler N, Nattermann J, Luedde T, Trautwein C, et al. Interleukin-8 is activated in patients with chronic liver diseases and associated with hepatic macrophage accumulation in human liver fibrosis. *PLoS One.* 2011; 6:e21381. [PubMed: 21731723]
30. Gabele E, Froh M, Arteel GE, Uesugi T, Hellerbrand C, Scholmerich J, et al. TNFalpha is required for cholestasis-induced liver fibrosis in the mouse. *Biochem Biophys Res Commun.* 2009; 378:348–353. [PubMed: 18996089]
31. Bahcecioglu IH, Koca SS, Poyrazoglu OK, Yalniz M, Ozercan IH, Ustundag B, et al. Hepatoprotective effect of infliximab, an anti-TNF-alpha agent, on carbon tetrachloride-induced hepatic fibrosis. *Inflammation.* 2008; 31:215–221. [PubMed: 18427963]
32. Choi I, Kang HS, Yang Y, Pyun KH. IL-6 induces hepatic inflammation and collagen synthesis in vivo. *Clin Exp Immunol.* 1994; 95:530–535. [PubMed: 8137551]
33. Chiramonte MG, Donaldson DD, Cheever AW, Wynn TA. An IL-13 inhibitor blocks the development of hepatic fibrosis during a T-helper type 2-dominated inflammatory response. *J Clin Invest.* 1999; 104:777–785. [PubMed: 10491413]
34. Kolodsick JE, Toews GB, Jakubzick C, Hogaboam C, Moore TA, McKenzie A, et al. Protection from fluorescein isothiocyanate-induced fibrosis in IL-13-deficient, but not IL-4-deficient, mice results from impaired collagen synthesis by fibroblasts. *J Immunol.* 2004; 172:4068–4076. [PubMed: 15034018]

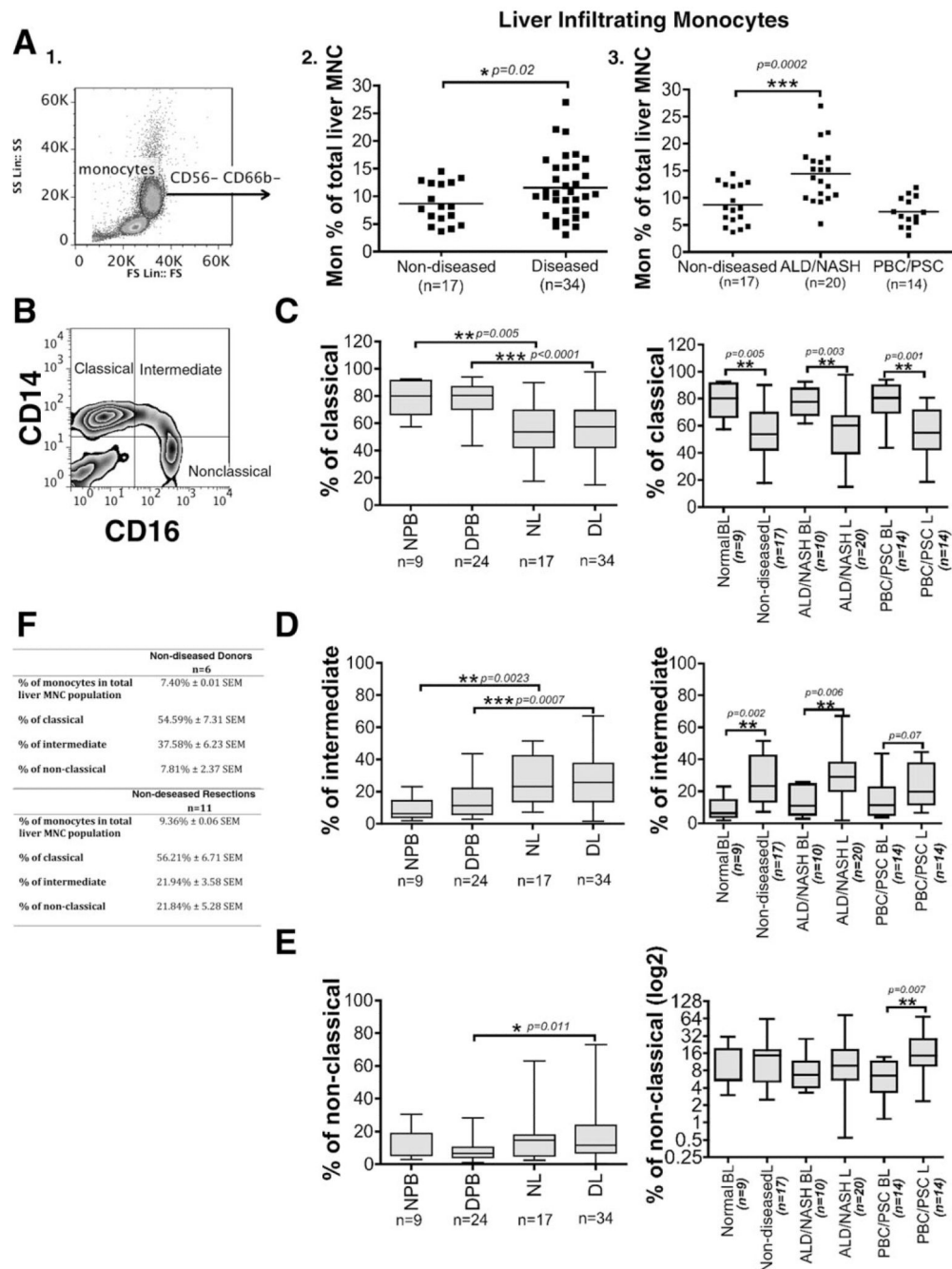


Fig. 1. Intrahepatic monocytes are expanded in human liver disease.

(A,1) Monocytes in blood and human liver were identified based on forward and side scatter and CD14/CD16 expression and exclusion of CD56+CD16+ NK cells and CD66b+CD16+ neutrophils (A,2 and A,3). The levels of monocytes were expressed as the percentage of total liver MNCs and were compared between nondiseased (donor and resections; n=17) and diseased livers (ALD [n = 17], NASH [n = 3], PBC [n = 8], and PSC [n = 6]). Each dot represents the value from each individual and the line represents the mean value ± SEM. Statistical analysis was performed via Student *t* test. **P* = 0.02, ****P* = 0.0002 versus

nondiseased livers. (B) Monocytes were further divided based on the CD14 and CD16 expression into classical (CD14⁺⁺CD16⁻), intermediate (CD14⁺⁺CD16⁺), and nonclassical (CD14⁺CD16⁺⁺) monocytes as shown by the representative quadrant flow cytometry plot. (C-E) The levels of classical (C, left panel), intermediate (D, left panel), and nonclassical (E, left panel) monocyte subsets are expressed as the percentage of total monocytes and were measured in normal peripheral blood (NPB [n = 9]), diseased peripheral blood (DPB [n = 24]), nondiseased livers (NL [n = 17]) and diseased livers (DL [n = 34]). The levels of classical (C, right panel), intermediate (D, right panel) and nonclassical (E, right panel) monocyte subsets were also recorded in the blood and liver of specific grouped etiologies: ALD/NASH and PBC/PSC. Horizontal bars represent the median values of the monocyte subset populations. Comparisons of the variables between the groups of blood and liver monocytes were made via Student *t* test. **P* < 0.05, ***P* < 0.01, ****P* < 0.001. (F) Table shows the percentage of monocytes in the total liver-infiltrating mononuclear cell population and the percentage of the three monocyte subsets in nondiseased donors (n = 6) and resections (n = 11). A Student *t* test revealed a significant difference (**P* = 0.03) in the levels of intermediate monocytes between donors and resections.

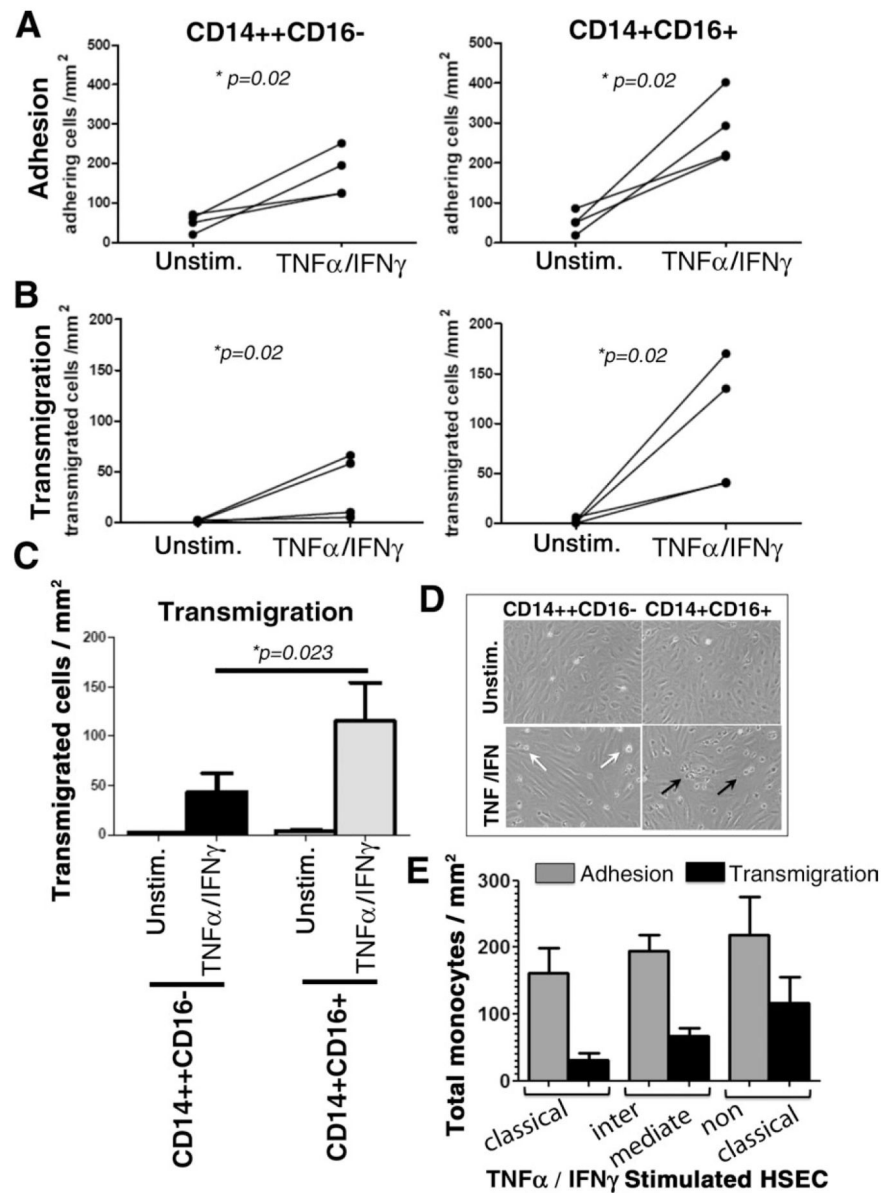


Fig. 2. Monocyte adhesion and transendothelial migration across cytokine-activated HSECs under physiological flow.

HSECs were grown to confluence in Ibidi chambers and stimulated with TNF α (10 ng/mL) and IFN γ (10 ng/mL) for 24 hours, after which either CD14⁺⁺CD16⁻ and CD14⁺CD16⁺ (comprising CD14⁺⁺CD16⁺ and CD14⁺CD16⁺⁺) subsets were perfused over the endothelial monolayer at a shear stress of 0.05 Pa. Adherent cells were classified as rolling, static (phase bright), or migrated (phase dark), and total adhesion was calculated. Experiments were repeated four times. (A,B) Data represent the changes of total CD14⁺⁺CD16⁻ and CD14⁺CD16⁺ monocytes adhering or transmigrated per mm² normalized to 10⁶ cells perfused. Studies were performed on resting or TNF α /IFN γ -activated HSECs. (C) Histograms depict total number of transmigrated CD14⁺⁺CD16⁻ and CD14⁺CD16⁺ monocytes/mm² normalized to 10⁶ cells perfused across HSECs with or without TNF α /

IFN γ stimulation. Statistical significance between subsets was calculated using a paired Student t test. (D) Representative images captured from experimental videos showing adherent (phase bright, white arrows) and migrated monocytes (phase dark, black arrows). (E) Data represent total adherent and total migrating cells over TNF α /IFN γ -stimulated HSECs. Classical, intermediate, and nonclassical monocyte subsets were acquired by cell sorting.

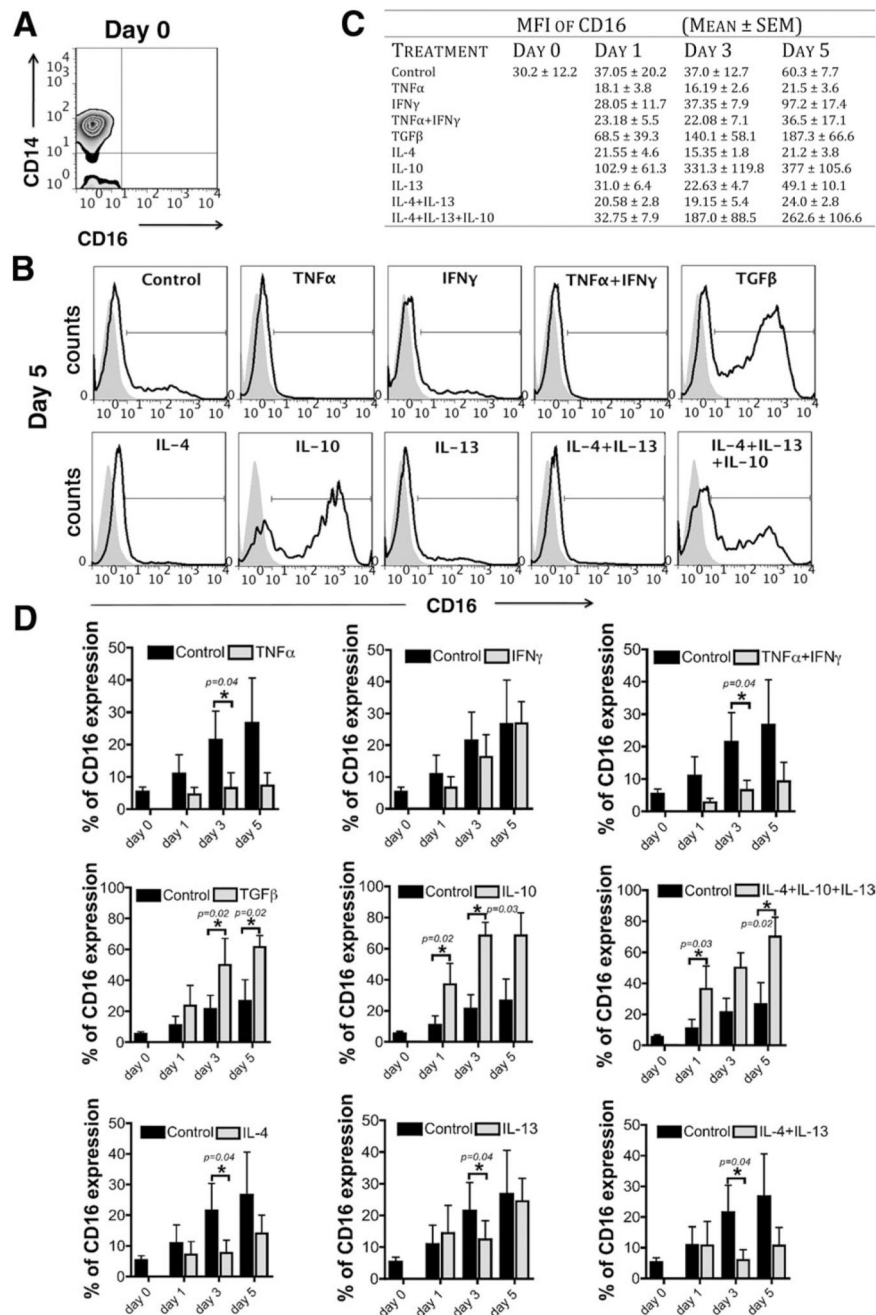


Fig. 3. Monocyte subset differentiation *in vitro*.

Human CD14⁺⁺CD16⁻ monocytes isolated from the blood of healthy volunteers were stimulated *in vitro* with TNF α (10 ng/mL), IFN γ (25 ng/mL), TNF α /IFN γ , TGF β (5 ng/mL), IL-4 (10 ng/mL), IL-10 (50 ng/mL), IL-13 (10 ng/mL), IL-4/IL-13 and IL-4/IL-13/IL-10 for 1, 3 and 5 days, and the expression of CD16 was studied by flow cytometry. (A) Representative quadrant flow cytometry plot showing the CD14⁺⁺CD16⁻ subset at day 0 after isolation. (B) Representative flow cytometry histograms showing the induction of CD16 expression on CD14⁺⁺CD16⁻ subset after 5 days of *in vitro* stimulation. (C) Table

shows the median fluorescence intensity (MFI) of CD16 expression (mean \pm SEM [n = 4]) at days 0, 1, 3, and 5. (D) Data show the percentage of CD16 expression on CD14⁺⁺CD16⁻ monocytes after 1, 3, and 5 days of stimulation with Th1 (TNF α , IFN γ), Th2 (IL-4, IL-13), or anti-inflammatory (IL-10, TGF β) cytokines (gray bars) compared with CD16 expression acquired by classical monocytes without stimulation (black bars; control). Statistical analysis was performed via Student *t* test.

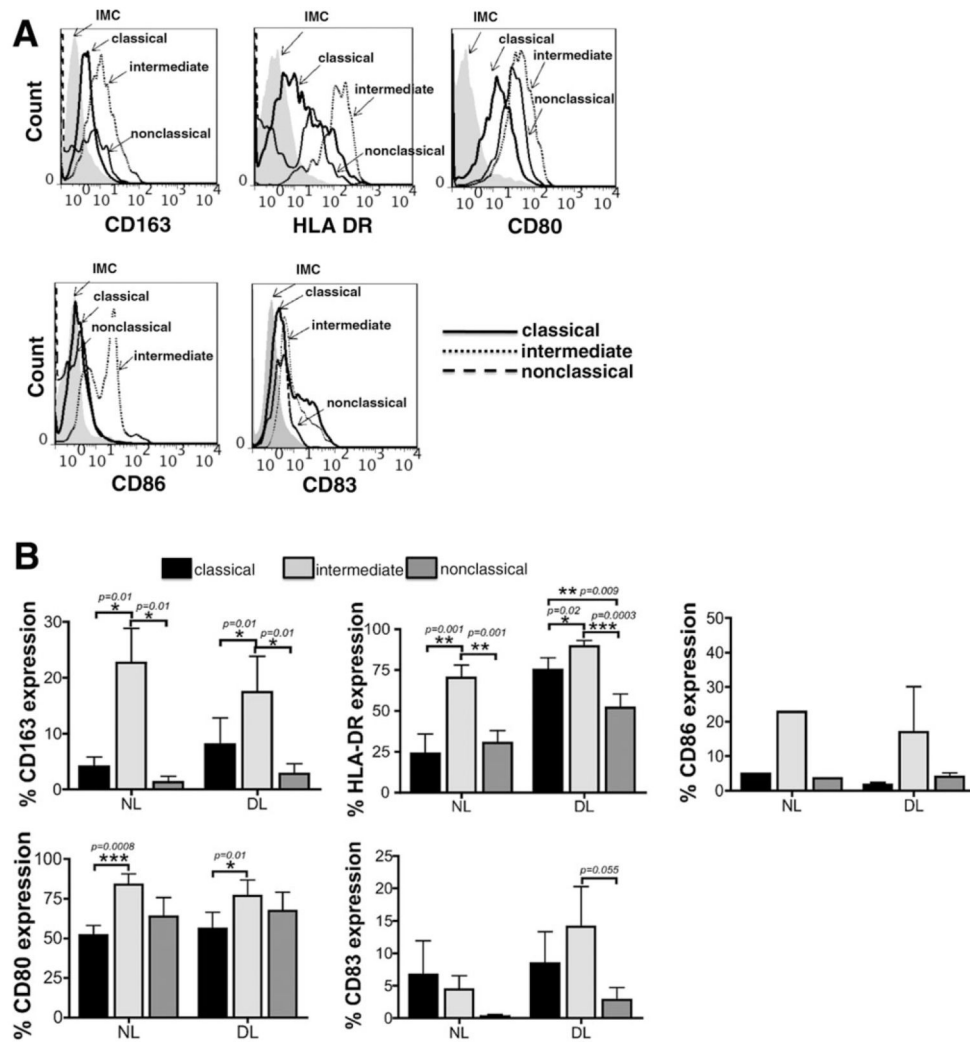


Fig. 4. Phenotypic characterization of monocyte subsets isolated from human liver. (A) Representative histogram plots of CD163, HLA-DR, CD80, CD86, and CD83 on classical, intermediate, and nonclassical liver-infiltrating monocyte subsets. IMC, isotype-matched control antibody. (B) Data representing the percentage of CD163, HLA-DR, CD80, CD83, and CD86 expression on classical, intermediate, and nonclassical monocytes derived from nondiseased livers (NL) (CD163 [n = 7], HLA DR [n = 6], CD80 [n = 4], CD83 [n = 5], and CD86 [n = 1]) and diseased livers (DL) (CD163 [n = 16], HLA DR [n = 15], CD80 [n = 9], CD83 [n = 12], and CD86 [n = 3]). * $P < 0.05$, ** $P < 0.01$, *** $P < 0.001$ (Student *t* test followed by Bonferroni's correction).

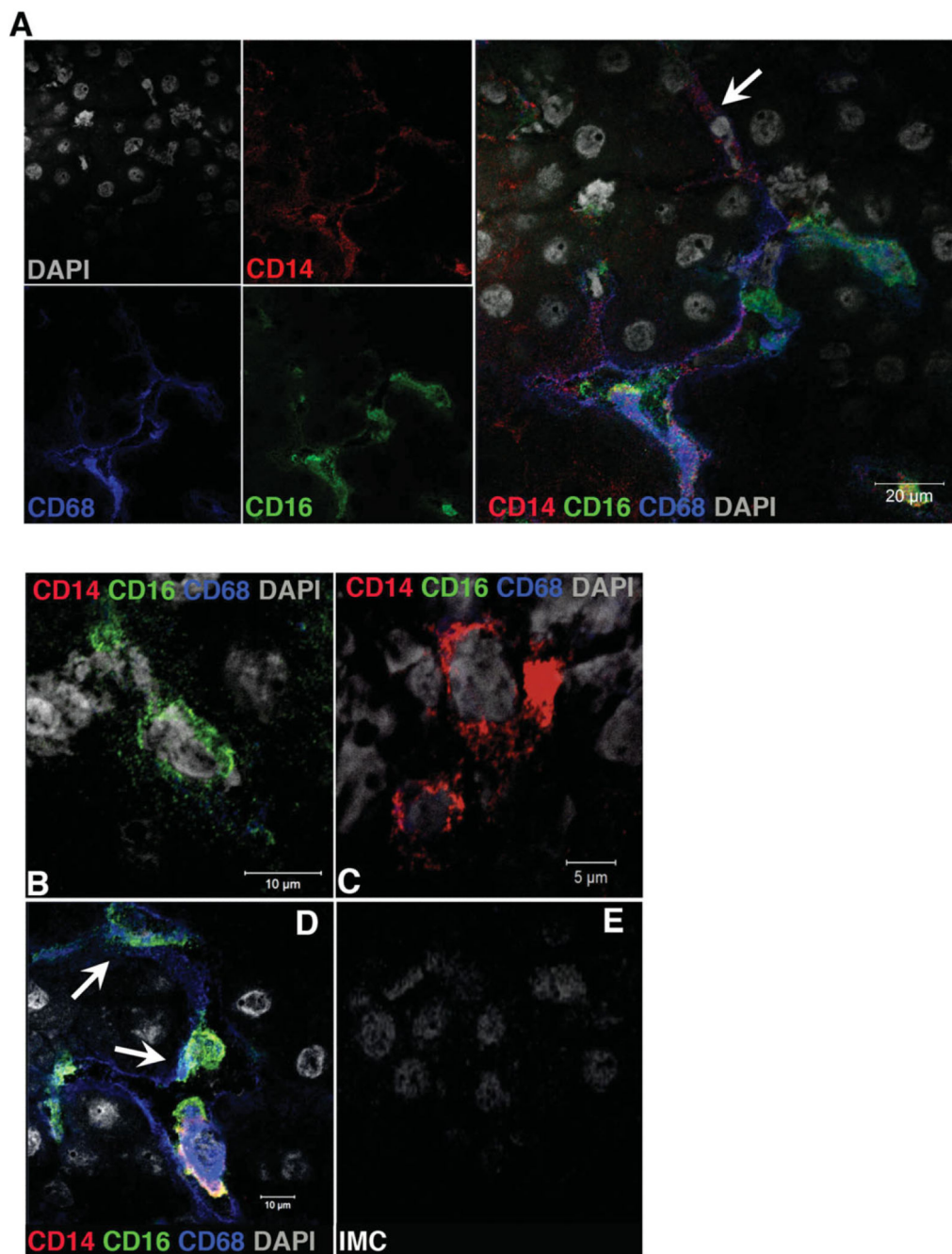


Fig. 5. Monocyte subset localization in human liver tissue.

The localization of monocyte subsets based on the expression of CD14 and CD16 and the expression of CD68 was tested by immunofluorescent staining. (A) Immunofluorescent staining images showing the colocalization of CD14+CD16+ monocytes with CD68+ liver macrophages along the hepatic sinusoids. Single positive CD16+ (B) and CD14+ (C) monocytes and CD14+CD68+ (A; white arrow) and CD16+CD68+ (D; white arrows) monocyte/macrophages are also detected in human liver tissue (red = CD14, green = CD16,

blue = CD68, and gray = DAPI). (E) Image showing staining with isotype matched control antibody (IMC). Images were acquired using a $\times 100$ oil objective.

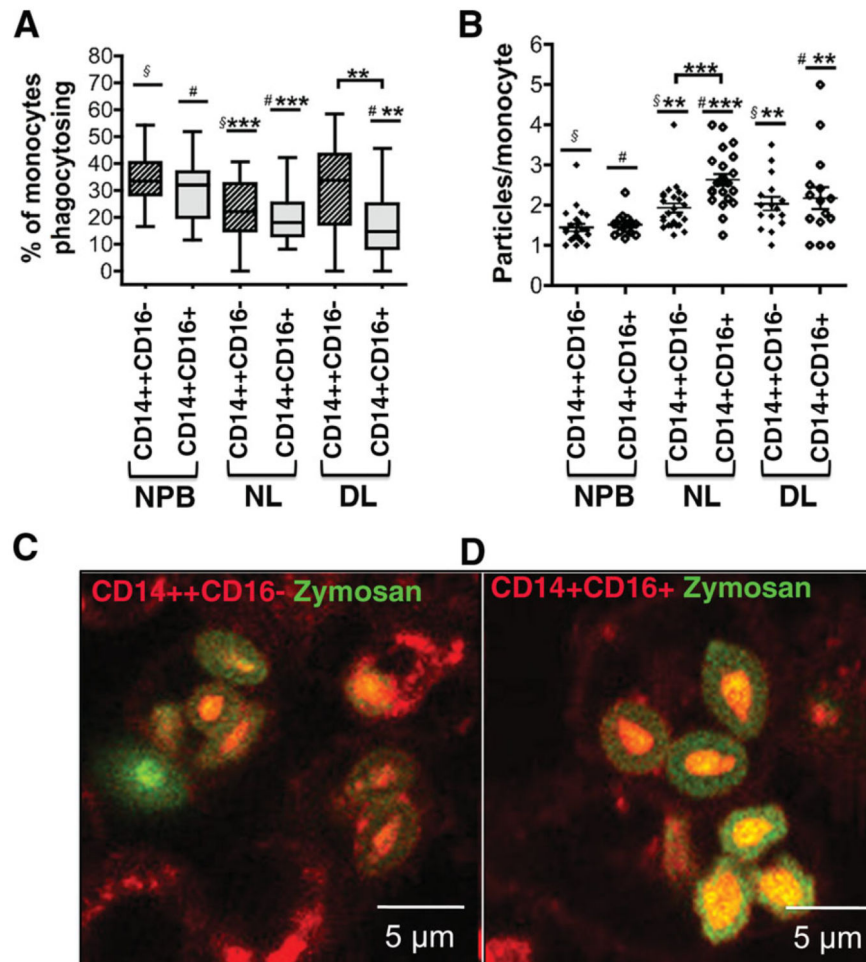


Fig. 6. Phagocytic capabilities of monocyte subsets.

The ability of monocyte subsets CD14⁺⁺CD16⁻ and CD14⁺CD16⁺ to phagocytose was tested using fluorescent-labeled zymosan bioparticles and was expressed as (A) percentage of monocytes that are able to phagocytose and (B) number of phagocytosed particles per monocyte (phagocytosis/monocyte). In the scatter dot plots presented, lines represents the mean \pm SEM. Statistical analysis was performed using a paired Student *t* test. DL, diseased liver (n = 1 ALD, n = 1 NASH, n = 1 PBC); NL, nondiseased liver (n = 3; normal resections); NPB, normal peripheral blood (n = 3) A) §*** vs § $P < 0.001$; #*** vs # $P < 0.001$; #** vs # $P < 0.01$ B) §** vs § $P < 0.01$; #*** vs # $P < 0.001$; #** vs # $P < 0.01$. (C,D) Representative confocal images showing monocytes in red and zymosan particles in green. The particles that have been phagocytosed are faint green because their fluorescence has been quenched.

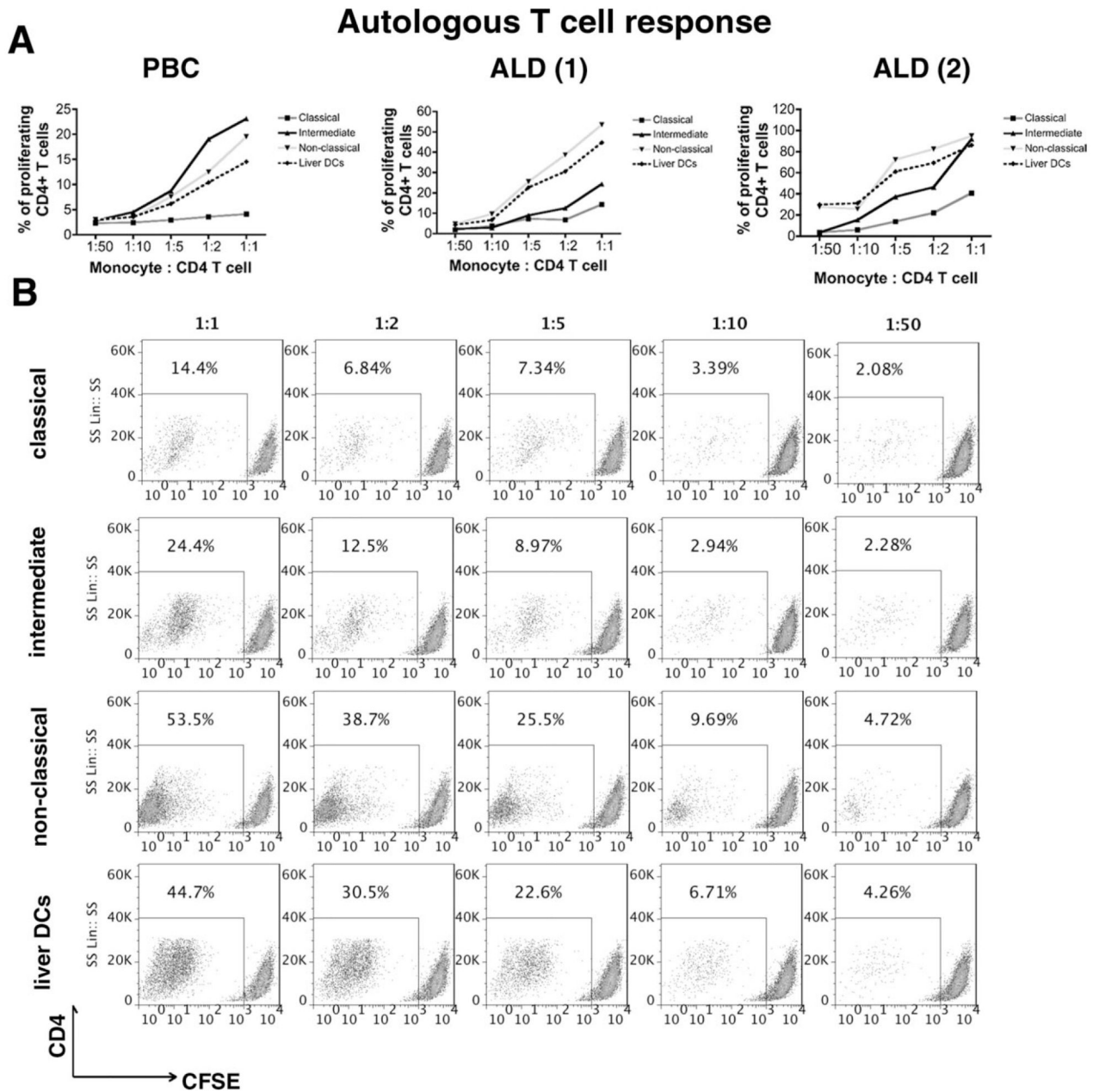


Fig. 7. Antigen presentation and T cell proliferation.

Classical, intermediate, and nonclassical monocytes and DCs isolated from three diseased human livers (ALD, n = 2; PBC, n = 1) by FACS were incubated with *tuberculosis* protein for 24 hours prior to coculturing with autologous CFSE-labeled CD4⁺ T cells for 4 days at 1:1, 1:2, 1:5, 1:10, and 1:50 ratios (monocyte/DC: CD4). (A) Percentage of proliferating CD4⁺ T cells at different coculture ratios in PBC and ALD livers. (B) Representative flow cytometry plots showing the T cell proliferation induced by the different monocyte subsets and liver DCs isolated from one of the two ALD livers. (1) and (2) represent the two different ALD livers tested.

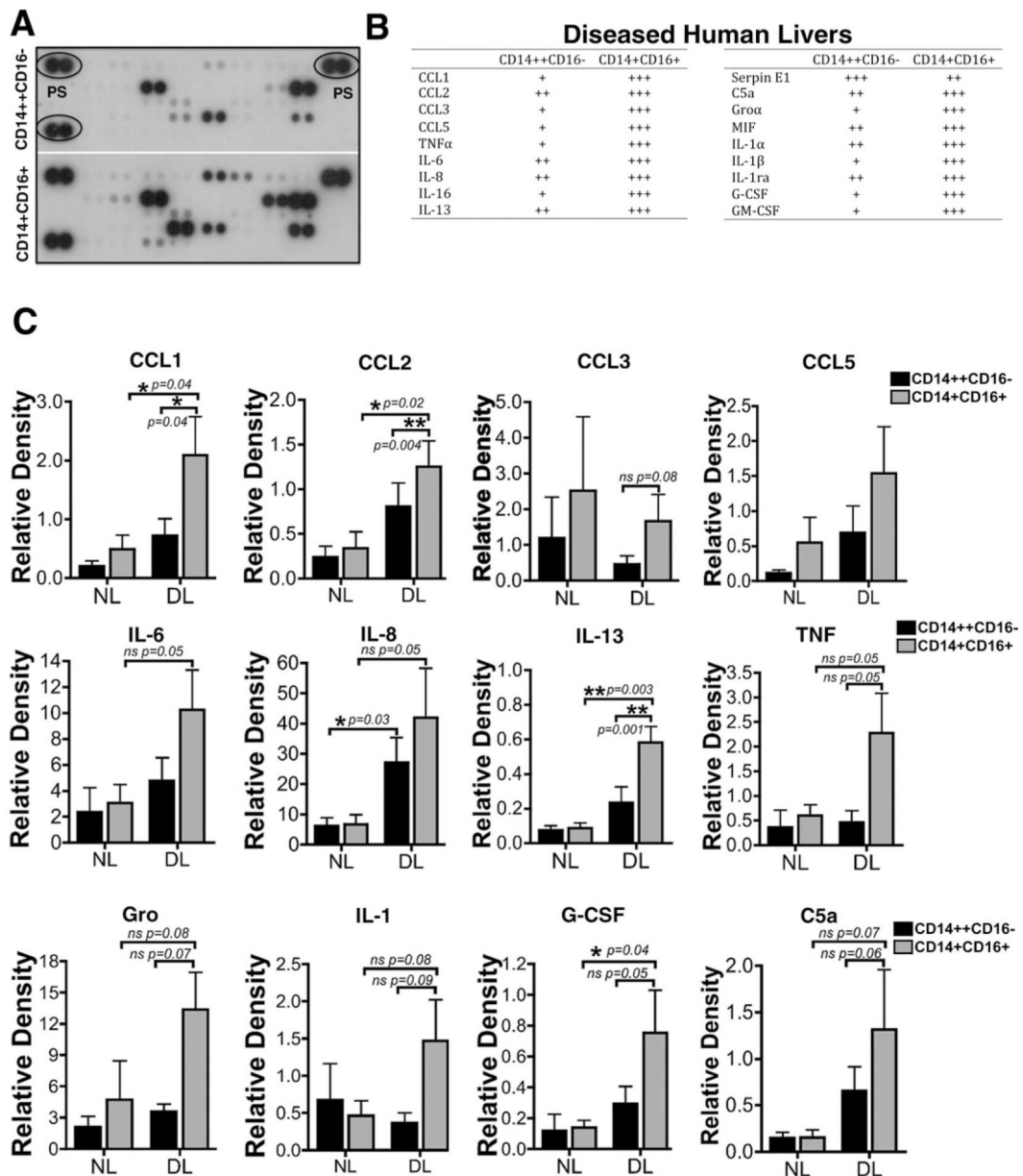


Fig. 8. Monocyte cytokine secretion analysis.

CD14++CD16⁻ and CD14+CD16⁺ monocytes isolated from nondiseased livers (n = 3) and diseased livers (ALD, n = 2; PSC, n = 1) were cultured for 48 hours prior to collection of conditioned media and analysis of cytokine secretion. (A) Representative dot plot image of cytokine array analysis showing the expression of different cytokines from CD14++CD16⁻ and CD14+CD16⁺ monocytes. PS, positive control. (B) Table shows the levels of cytokines secreted by diseased livers infiltrating CD14++CD16⁻ and CD14+CD16⁺ monocytes. (C) Cytokines released by nondiseased and diseased liver-infiltrating monocytes relative to positive controls, all normalized to 10⁶ cells. **P* < 0.05, ***P* < 0.01, ****P* < 0.001 (paired Student *t* test).